An Arithmetic Optimization Algorithm for the Optimal Deployment of Electric Vehicle Fast Charging Stations in the Distribution Network with PV Integration

Khoa Hoang Truong
Department of Power Delivery, Ho Chi Minh City University of Technology (HCMUT), Dien Hong Ward, Ho Chi Minh City, Vietnam | Vietnam National University Ho Chi Minh, Linh Xuan Ward, Ho Chi Minh City, Vietnam
trhkhoa@hcmut.edu.vn

Dieu Ngoc Vo
Department of Power Systems, Ho Chi Minh City University of Technology (HCMUT), Dien Hong Ward, Ho Chi Minh City, Vietnam | Vietnam National University Ho Chi Minh, Linh Xuan Ward, Ho Chi Minh City, Vietnam
vndieu@hcmut.edu.vn

Hung Duc Nguyen
Department of Power Delivery, Ho Chi Minh City University of Technology (HCMUT), Dien Hong Ward, Ho Chi Minh City, Vietnam | Vietnam National University Ho Chi Minh, Linh Xuan Ward, Ho Chi Minh City, Vietnam
hungnd@hcmut.edu.vn (corresponding author)

Received: 4 September 2025 | Revised: 12 October 2025 | Accepted: 18 October 2025

 DOI: https://doi.org/10.48084/etasr.14524

ABSTRACT

Electric Vehicles (EVs) have attracted significant interest from the automotive sector and government bodies due to their lower carbon dioxide emissions and reduced maintenance and operational expenses. However, the increasing adoption of EVs impacts distribution network factors, including power losses and voltage stability. To ensure network reliability, it is crucial to strategically locate EV Fast-Charging Stations (EV-FCSs). This study presents a two-stage approach for optimal FCS placement. In Stage 1, a Charging Station Owner Decision Index (CSODI) is proposed to identify cost-effective locations with high EV traffic. In Stage 2, an Enhanced Arithmetic Optimization Algorithm (EAOA) is applied to minimize real power loss and investment costs, while ensuring that system constraints are met. The proposed method is validated using the IEEE 34-bus distribution system under two scenarios: one without Vehicle-to-Grid (V2G) and the other with V2G. Further analysis considers three subcases: optimizing for investment cost (Case 1), a balanced trade-off (Case 2), and power loss minimization (Case 3). The results demonstrate that V2G significantly reduces power loss and improves voltage stability across all cases, with Case 2 offering the best balance between cost and efficiency. The findings confirm that optimized FCS placement, coupled with V2G and renewable integration, enhances grid performance, sustainability, and cost efficiency in modern distribution networks.

Keywords-distribution networks; electric vehicles; fast charging stations; distributed generation

I. INTRODUCTION

The integration of Distributed Generation (DG) and Electric Vehicle Charging Stations (EVCSs) is transforming power networks. Solar-based DG (SDG) is gaining popularity due to its environmental benefits, cost reductions, and technological advancements, enabling decentralized energy production and improving voltage stability. Renewable energy technologies also promote the expansion of EVs, reducing reliance on fossil fuels and lowering greenhouse gas emissions. EVs offer benefits such as zero emissions, lower running costs, and reduced noise pollution. However, widespread EV adoption

depends on adequate charging infrastructure, categorized into three levels based on power and charging speed. While EVCSs support grid stability through V2G integration, unplanned EVCS deployment can cause power losses, voltage fluctuations, and grid instability. Strategic placement of EVCSs is essential to mitigate these issues and ensure a reliable power distribution network.

The optimization of Fast Charging Station (FCS) placement has been approached using various techniques, with objectives such as reducing development costs and minimizing power loss. Authors in [1] applied the balanced mayfly technique to determine the optimal FCS locations. Authors in [2] formulated a multi-objective optimization problem that considered substation energy loss costs, installation costs, and conveyance energy loss, which were solved with the binary lightning search algorithm. Furthermore, authors in [3] proposed an optimization model that considers land costs, EV fleet distribution, voltage fluctuations, and energy losses as key objectives. To address the uncertainties associated with EV demand, the study employed the 2m Point Estimation Method (2m PEM), while the Harris Hawks optimization technique was used to obtain the optimal solution.

Further efforts in optimizing FCS placement have incorporated a wider range of factors, including station investment costs, energy consumption costs of EVs, network power losses, and voltage deviations. To address this challenge, a novel hybrid Shuffled Frog Leap-Teaching Learning-Based Optimization (SFL-TLBO) method was introduced in [4]. Authors in [5] formulated the problem using objective functions such as power loss reduction, voltage stability, and EV charging costs. In [6], the bat algorithm was applied to minimize electrical power losses and determine optimal charging zone centers for FCS placement.

Other approaches [7] include an improved whale optimization algorithm for siting and sizing EVCSs based on traffic patterns and area segmentation. In [8], a comprehensive model was developed to optimize charging station placement by considering operational expenses, overall investment, and charging costs, while also integrating energy storage and renewable energy. In [9], the optimization of EV-FCS placement was addressed by minimizing power losses in an imbalanced Radial Distribution Network (RDN) based on a Particle Swarm Optimization (PSO). Authors in [10] defined optimum parking lot allocation by maximizing income while considering power loss costs, reliability, and voltage deviation, and optimal solutions were obtained by a Genetic Algorithm (GA). In [11], active power loss and installation costs were incorporated in the objective function, which was solved using the Grey Wolf Optimizer (GWO). Authors in [12] optimized FCS allocation for sustainable cities, considering operation cost, construction cost, travel cost, and annualized time opportunity cost, with GA applied to solve the problem. In [13], the optimal locations for capacitors and FCSs were determined by considering the costs of power losses. Authors in [14] analyzed the impact of CS and DG placement on distribution system reliability, where power loss and voltage deviation costs were optimized using a hybrid GWO–PSO approach. In [15], reliability indices, power loss, and voltage deviation for CS placement were evaluated using a metaheuristic algorithm implemented in MATLAB/Simulink. Many metaheuristics have been applied to the optimal placement problem, such as bald eagle search [16], hybrid gray wolf optimizer-particle swarm optimizer [17], equilibrium optimizer [18], and symbiotic organisms search [19].

Previous studies have focused on optimizing the deployment of FCS. Nevertheless, no existing approach has simultaneously considered land cost, EV population, and V2G integration within the multi-objective optimization framework. This paper presents a novel methodology for FCS placement by incorporating these factors, along with investment cost and power losses.

The proposed method can enhance the system efficiency by balancing the charging station owner's priorities with distribution network constraints to achieve optimal loss reduction. The proposed method follows a two-stage optimization process. The first stage introduces the CSODI to rank potential FCS locations, maximizing EV accessibility while minimizing land costs. In the second stage, investment cost and power losses are minimized to identify the most suitable FCS placements. Additionally, installation costs, distribution system quality improvements, and profitability are factored into the decision-making process. To further alleviate grid stress, Solar-Powered Distributed Generation (SPDG) units are integrated at various strategic locations. Furthermore, an EAOA is introduced by integrating the Simple Quadratic Interpolation (SQI) strategy to solve the formulated optimization problem.

The proposed approach was evaluated using the IEEE 34-bus distribution network and compared with other optimization techniques. The results of the comparative analysis demonstrate the superior performance of the proposed method over other methods, confirming the EAOA's efficiency and effectiveness in determining the optimal placement of EV_FCS.

II. PROBLEM FORMULATION

This research presents a methodology for optimal FCS placement by minimizing power losses and investment costs while satisfying distribution network constraints. To achieve this, the CSODI is developed, incorporating key factors such as land cost and EV population. Additionally, an objective function is formulated while considering various network constraints. Furthermore, EV loads are integrated with V2G strategies to enhance system efficiency. Land costs in urban areas can be extremely high and vary significantly within the same city. As a result, FCS investors prioritize land expenses when selecting locations. At the same time, accessibility is crucial, requiring investors to assess EV population density at potential sites to maximize profitability.

A. Number of Fast Charging Stations

The number of FCSs (N_{FCS}) for the selected case study region was determined to meet charging demands efficiently:

$$N_{FCS} = \frac{p^{EV} \cdot N^{EV} \cdot Ch_{time}}{S_t \cdot Ef \cdot C_p \cdot N^C \cdot pf} \quad (1)$$

where p^{EV} represents the average power demand of EVs, N^{EV} denotes the number of EVs charged daily, and Ch_{time} refers to the charging duration. Additionally, S_t is the charger service time, N^C represents the number of connectors per FCS, and C_p indicates the connector capacity. The equation also accounts for *Ef* (charging efficiency) and *pf* (charging load power factor) to ensure accurate estimation.

B. Charging Station Owner Decision Index

Urban land prices are often high and can vary significantly within a city. As a result, FCS investors prioritize evaluating land costs at potential locations. Every bus in the distribution system is evaluated for FCS placement, and a Land Cost Index (LCI) is introduced to incorporate land expenses into the optimization process. The normalized LCI is calculated by dividing the land cost of each bus by the highest land cost among all buses, resulting in values ranging from 0 to 1:

$$LCI_i^{NB} = \frac{LC_i^{NB}}{\max(LC_i^{NB})} \quad (2)$$

where *NB* is the number of buses, and LC_i denotes the land cost for the i^{th} bus.

Investor profit is directly linked to the number of EVs charged at an FCS, making the EV population at each bus a key factor. To identify optimal locations, the Electric Vehicle Flow Index (EVFI) can be applied, ranking buses based on EV density. The normalized EVFI is calculated by dividing the EV count at each bus by the highest EV count among all buses and is expressed as:

$$EVFI_i^{NB} = \frac{EVF_i^{NB}}{\max(EVF_i^{NB})} \quad (3)$$

where EVF_i is the EV population at the i^{th} bus.

The *CSODI*, formulated to balance land cost and EV population, combines the normalized *LCI* and *EVFI* as:

$$CSODI_i^{NB} = \alpha \cdot LCI_i^{NB} - \beta \cdot EVFI_i^{NB} \quad (4)$$

where α and β are positive coefficients adjusting the weight of each factor, both set to 0.5. Based on *CSODI*, investors prioritize FCS placement at buses that: (1) offer lower land costs, making installation more affordable; (2) have a high EV population, maximizing charging demand and profitability.

C. EV Load Modeling with V2G Strategies

Advancements in power electronics have enabled FCS converters to achieve bidirectional power flow. In G2V mode, power flows from the grid to the vehicle battery during charging, while in V2G or V2H mode, power is discharged back to the grid or home. This paper focuses on V2G mode due to its benefits for both the distribution system and EV users. The EV-FCS load demand with V2G integration is formulated as:

$$P_{FCS,j} = \begin{cases} N_{EV}^{G2V} \cdot R_{ch} - N_{EV}^{V2G} \cdot R_{dis} & \text{if } Z_j = 1 \\ 0 & \text{if } Z_j = 1 \end{cases} \quad (5)$$

where Z_j is a binary variable for FCS placement, N_{EV}^{G2V} and N_{EV}^{V2G} represent the number of EVs in G2V and V2G modes, respectively, and R_{ch} and R_{dis} are the EV battery charging and discharging rates.

D. Formulation of Optimization Problem

1) Investment Cost Reduction Indicator

Land cost varies by location and significantly impacts the project's total expenses, along with development costs. However, as technology advances, these costs are expected to decrease. Therefore, FCS investors must assess land costs at the potential locations. The Investment Cost (IC) is calculated by combining fixed costs, land costs, and connector development costs, as defined in (6). Each FCS requires a minimum area of 100 m², and the land cost is calculated based on a five-year rental period. To standardize the investment costs, the IC Reduction Indicator (ICRI) is introduced in (7).

$$IC_i = C^{fix} + 100 N_D \cdot C_{land,i} + (N_C - 1) C_p \cdot C_{dev} \quad (6)$$

$$ICRI_i = 1 - \frac{IC_i}{\max(IC_i)} \quad (7)$$

where C^{fix} is the fixed charger installation cost, $C_{land,i}$ is the land rental cost per m² per day (over five years) at bus *i*, C_p is the rated power of the connector, N_C is the number of connectors, C_{dev} is the development cost per connector, and N_D is the number of planning days.

2) Real Power Loss Reduction Indicator

The active Power Loss Reduction Indicator (*PLRI*) helps identify optimal FCS locations by assessing potential grid power loss increases upon FCS integration as:

$$PLRI = 1 - \frac{P_{L,base}}{P_L} \quad (8)$$

where $P_{L,base}$ is the total real power loss without FCS placement, and P_L is the total real power loss with FCS placement. Additionally, the real active power loss is calculated by:

$$P_L = \sum_{l=1}^{NL} R_l I_l^2 \quad (9)$$

where *NL* is the number of branches, I_l is the current through the l^{th} branch, and R_l is the resistance of the l^{th} branch.

3) Objective Function

The goal is to minimize real power loss and investment costs for optimal FCS placement, which is formulated as an optimization problem:

$$f = \omega_1 \cdot PLRI + \omega_2 \cdot \sum_{i=1}^{NB} \left(\frac{ICRI_i \cdot Z_i}{N_{FCS}} \right) \quad (10)$$

where ω_1 and ω_2 are weighting factors to balance power loss reduction and investment cost in decision-making.

4) Constraints

For the optimal site of FCSs, the expressed cost function must adhere to some inequality and equality restrictions.

1. Real power balance

In an RDN, the power balance is defined by:

$$P_{SS} + \sum_{n=1}^{N_{DG}} P_{DG,n} = \sum_{i=1}^{N_B} P_{D,i} + \sum_{l=1}^{N_L} P_{L,l} + \sum_{j=1}^{N_{FCS}} P_{FCS,j} \quad (11)$$

$$Q_{SS} + \sum_{n=1}^{N_{DG}} Q_{DG,n} = \sum_{i=1}^{N_B} Q_{D,i} + \sum_{l=1}^{N_L} Q_{L,l} + \sum_{j=1}^{N_{FCS}} Q_{FCS,j} \quad (12)$$

where P_{SS} and Q_{SS} are powers injected from the reference bus, $P_{D,i}$ and $Q_{D,i}$ represent power demands at i^{th} bus without FCS integration, $P_{L,l}$ and $Q_{L,l}$ represent power losses in the l^{th} branch, $P_{FCS,j}$ and $Q_{FCS,j}$ are the active and reactive power of the j^{th} FCS, $P_{DG,k}$ and $Q_{DG,k}$ represent the power generated from the n^{th} DG unit, N_{DG} is the number of DG units, and N_B is the number of buses.

2. Voltage constraints

The load bus voltage magnitude (V_i) is given by:

$$V_{\min,i} \le V_i \le V_{\max,i} \; ; \; \forall i = 1,...,N_B \quad (13)$$

where $V_{min,i}$ and $V_{max,i}$ denote the minimum and maximum voltage limits at the i^{th} bus, respectively.

3. Current constraints

The current flowing through a line (I_l) should not exceed the limited capacity:

$$|I_l| \le |I_{\max,l}| \; ; \; \forall l = 1,...,N_L \quad (14)$$

where $I_{max,l}$ denotes the maximum loading of the l^{th} branch.

4. Placement of EVCS constraint

EVCS placement is determined by the *CSODI* in (4). The *LCI*, *EVFI*, and *CSODI* values are calculated and ranked in ascending order, with the top 12 locations selected for FCS installation.

III. ENHANCED ARITHMETIC OPTIMIZATION ALGORITHM

A. Arithmetic Optimization Algorithm

1) Population Initialization

As proposed in [20], AOA starts the optimization process with a randomly generated set of candidate solutions (X), as depicted in:

$$X = \begin{bmatrix} x_{1,1} & \cdots & x_{1,j} & \cdots & x_{1,n} \\ x_{2,1} & \cdots & x_{2,j} & \cdots & x_{2,n} \\ \vdots & \vdots & \vdots & \vdots & \vdots \\ x_{N,1} & \cdots & x_{N,j} & \cdots & x_{N,n} \end{bmatrix} \quad (15)$$

where N is the population size, n is the problem dimension, and $x_{i,j}$ indicates the j^{th} position of the i^{th} solution.

Prior to the initialization of the search, a Math Optimizer Accelerated (MOA) function can be calculated as:

$$MOA(k) = Min + k\left(\frac{Max - Min}{k^{\max}}\right) \quad (16)$$

where *Min* and *Max* denote the minimum and maximum values of the *MOA* function, respectively, and variables k and k^{max} denote the current iteration and the total number of iterations, respectively.

2) Exploration Phase

Exploration mechanisms are represented by the Division (D) or Multiplication (M) operators. Specifically, if $r2 < 0.5$, the D operator is employed. Otherwise, the M operator is used. These strategies are executed to identify and update the optimal solution according to:

If $r1 > MOA(k)$, then:

$$x_{i,j}(k+1) = \begin{cases} \frac{best(x_j)}{MOP + \varepsilon} \cdot \left[(UB_j - LB_j) \cdot \mu + LB_j\right], \\ r2 < 0.5 \\ \text{best}(x_j) \cdot MOP\left[(UB_j - LB_j) \cdot \mu + LB_j\right], \\ \text{otherwise} \end{cases} \quad (17)$$

$$MOP(k) = 1 - \left(\frac{k}{k^{\max}}\right)^{\frac{1}{a}} \quad (18)$$

where $best(x_j)$ indicates the j^{th} position in the best solution; $x_{i,j}(k+1)$ indicates the j^{th} position of the i^{th} solution in the next iteration. LB_j and UB_j denote the boundaries of the j^{th} position, respectively; $r1$ and $r2$ are random numbers distributed in [0,1]; μ is a control parameter for the search process; ε is a small integer value; and Math Optimizer Probability (*MOP*) is a coefficient, with $MOP(k)$ representing the functional value at the k^{th} iteration. The AOA algorithm stops once the termination criterion is met. The flowchart of the AOA is illustrated in Figure 1.

3) Exploitation Phase

In this stage, subtraction and addition operators are utilized to potentially capture optimal solutions. This process proceeds according to the conditional criteria of the *MOA*, ensuring that it is not greater than the current iterative *MOA* values at $r1$ ($r1 \le MOA(t)$). Additionally, these two operators help identify dense areas to determine the best solution effectively. This process can be guided by two primary search techniques, which are modeled as:

$$x_{i,j}(k+1) = \begin{cases} best(x_j) - MOP\left[(UB_j - LB_j) \cdot \mu + LB_j\right], \\ r3 < 0.5 \\ \text{best}(x_j) + MOP\left[(UB_j - LB_j) \cdot \mu + LB_j\right], \\ \text{otherwise} \end{cases} \quad (19)$$

where r3 indicates a random number in [0,1].

In AOA, the roles of r1, r2, and r3 are to balance exploration and exploitation, with r1 scaling the exponential term controlling convergence speed, r2 regulating the influence of equilibrium candidates, and r3 randomizing the search direction to improve diversity. These parameters are re-initialized at every iteration, ensuring the stochasticity and robustness of the optimization process.

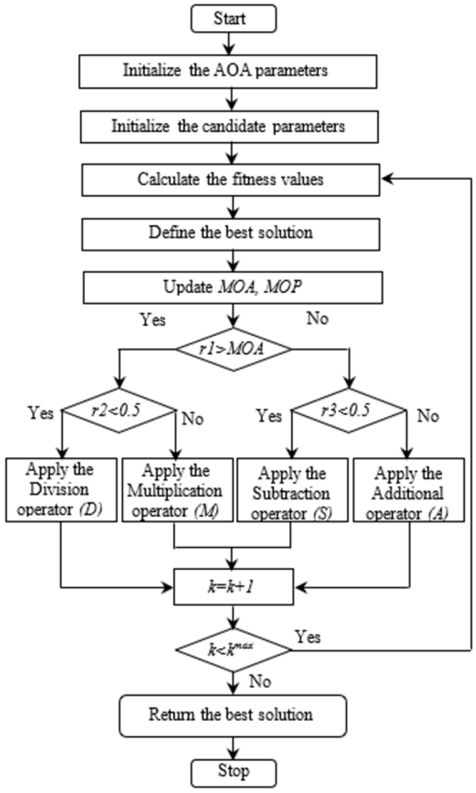

Fig. 1. Flowchart of the AOA.

B. Simple Quadratic Interpolation Strategy

As part of EAOA, the SQI approach is integrated to enhance searchability. At each iteration, a three-point SQI can be used to define the dimensions of a new candidate solution following the AOA optimization phase:

$$X_k^{New} = \frac{f_n(X_{k,d}^2 - X_{m,d}^2) + f_k(X_{m,d}^2 - X_{n,d}^2) + f_m(X_{n,d}^2 - X_{k,d}^2)}{f_n(X_{k,d} - X_{m,d}) + f_k(X_{m,d} - X_{n,d}) + f_m(X_{n,d} - X_{k,d})} \quad (20)$$

where X_m and X_n are random solutions selected from the population, f_k, f_m, and f_n are Fitness Functions (*FFs*) corresponding to k^{th}, m^{th}, and n^{th} solutions, respectively, and d = 1,…, n. If X_k^{New} has a better *FF* value than the current solution X_k, it replaces the current solution in the population.

C. Implementation of EAOA to the EVCS Placement Problem

The EAOA application for the EVCS placement problem is described by:

- Step 1: Set the variable boundaries and the number of charging stations (N_{FCS}).
- Step 2: Set the EAOA parameters, including N and k^{max}.
- Step 3: Randomly initialize a population of EAOA according to (15).
- Step 4: For each particle in the initial population, run the power flow and calculate the *FF*. Assign Iter to 0:

$$FF = f + K_V \sum_{i=1}^{N_B} (V_i - V_i^{\lim})^2 + K_I \sum_{i=1}^{N_B} (I_l - I_l^{\lim})^2 \quad (21)$$

where f is the fitness function, K_V and K_I are the penalty factors for the bus voltages and branch currents, and V_i^{lim} and I_l^{lim} are the limitations for the i^{th} bus voltages and l^{th} branch current.

- Step 5: Increment the iteration counter. Identify the best solution so far.
- Step 6: Update the MOA value based on (16).
- Step 7: Position updating in the Exploration phase using (17). Update the MOP value based on (18).
- Step 8: Updating of the Exploitation phase using (19).
- Step 9: Perform SQI according to (20).
- Step 10: If $k \leq k^{max}$, return to Step 5. Otherwise, terminate the optimization procedure.

IV. RESULTS

The proposed EAOA method was implemented to determine the optimal placement of FCSs in a 34-bus distribution system. As solar-based DGs continue to grow as a key renewable energy source, their integration helps balance the disparity between the power demand and generation caused by FCS deployment. To alleviate grid stress from EV loads, solar-based DGs were randomly placed across the distribution network, as detailed in Table I.

TABLE I. DATA FOR SOLAR-BASED DGS

DG no.	Bus	Real power (kW)	Reactive power (kVar)
1	5	840	276
2	16	1120	368
3	22	184	184

Table II outlines the land rental costs per m² per day and the EV population at potential EV-FCS locations within the IEEE 34-bus system. The land cost data used in this study are taken from [11]. Locations without available land for FCS installation were marked as infeasible by assigning them an infinite value. Every bus, except the slack bus, was considered for FCS placement.

TABLE II. LAND COSTS AND EV POPULATION

Bus no.	Land cost	EV population	Bus no.	Land cost	EV population
1	Inf	0	18	0.3	170
2	0.12	10	19	0.5	200
3	0.2	100	20	0.4	30
4	0.5	20	21	0.12	20
5	Inf	30	22	Inf	20
6	0.5	30	23	0.5	10
7	0.5	40	24	0.4	10
8	0.6	40	25	0.15	10
9	0.6	50	26	0.5	10
10	0.12	50	27	0.4	30
11	Inf	50	28	0.3	30
12	0.4	50	29	0.1	20
13	0.15	60	30	0.3	20
14	0.14	80	31	0.4	20
15	0.12	100	32	0.12	20
16	Inf	120	33	0.6	10
17	0.4	150	34	0.5	10

Table III presents the key parameters for FCV deployment. The study assumes that 1000 EVs are charged daily within the target area. Each EV-FCS is equipped with five connectors, requiring a total of four EV-FCSs to meet demand, as calculated in (1).

TABLE III. PARAMETERS FOR FCS DEPLOYMENT

Parameters	Value	Parameters	Value
Average power demand of EV (pEV)	96 kW	Number of connectors in FCS (NC)	5
Number of EVs (NEV)	1000	Charging load power factor (pf)	0.95
Charging duration (Chtime)	0.33 h	Fixed charger installation cost (Cfix)	21900 $
Charger service time (St)	18 h	Development cost per connector (Cdev)	109.5 $
Charging efficiency (Ef)	0.9	Number of days (ND)	1825
Connector capacity (Cp)	100 kVA		

A. CSODI Analysis

As outlined above, the *CSODI* was calculated for each bus in the distribution system. The *CSODI* values were then ranked in ascending order, prioritizing buses with low land costs and high EV populations for FCS placement, as shown in Table IV. In the first stage, this approach significantly reduced the search space for the optimization problem by identifying the most suitable FCS locations. Additionally, both the land cost and EV population were integrated into the decision-making process to ensure optimal placement within the distribution network. As a result, the number of potential FCS locations was reduced from 33 to 15. Finally, the four best locations were selected by minimizing investment costs and power losses while adhering to system constraints.

TABLE IV. CSODI VALUES OF POTENTIAL LOCATIONS FOR FCS DEPLOYMENT

Bus no.	*CSODI*	Bus no.	*CSODI*
18	-0.175	29	0.0333
15	-0.15	21	0.05
14	-0.0833	32	0.05
3	-0.0833	2	0.075
19	-0.0833	25	0.1
17	-0.0416	28	0.175
10	-0.025	30	0.2
13	-0.025		

B. Results of Optimal FCS Deployment

This study explores two scenarios for EV-FCS placement, aiming to minimize power losses and installation costs:

- Scenario 1: Identifies the optimal EV-FCS locations without V2G integration.
- Scenario 2: Determines the optimal EV-FCS locations with V2G strategies, where 10% of EVs participate in V2G, and each EV-FCS has one V2G-enabled connector.

In each scenario, three subcases were analyzed by adjusting the weighting factors ω_1 and ω_2 to evaluate their impact on the optimization process. In the base case, where EV-FCS are not installed in the IEEE 34-bus system, the total active power loss in the distribution lines is 165.3674 kW, and the minimum voltage is 0.9518 at bus 27.

For the EAOA algorithm, the control parameters were set to $N = 50$ and $k^{max} = 100$, with 10 independent trials conducted on the MATLAB platform. The selection of these parameters was guided by prior literature, following typical settings reported in recent applications of metaheuristics for power system optimization in [21, 22]. Power flow calculations were performed using Matpower 6.0.

1) Scenario 1

In this scenario, the optimal locations of the charging stations are determined without the V2G strategy, and three different cases were evaluated to analyze the impact of varying weighting factors (ω_1 and ω_2), as displayed in Table V.

In Case 1, the objective function prioritizes minimizing investment costs while disregarding power loss. Consequently, the *ICRI* value is 0.4897, and the power loss reaches 248.8810 kW. The power loss is significantly higher than in other cases, indicating that cost-effective locations may not always contribute to system efficiency. In Case 2, the optimization problem equally balances power loss reduction and investment cost minimization. The *ICRI* value and power loss are 0.5081 and 199.7480 kW, respectively. The results show a more significant drop in power loss than in the previous case (Case 1), but with a moderate increase in investment cost. In Case 3, power loss is slightly reduced to 197.0236 kW, the lowest among all cases, but at the highest investment cost (*ICRI* = 0.5291). In this case, the selected FCS locations are more focused on grid efficiency rather than cost-effectiveness. The optimal choice depends on stakeholder priorities. If cost is a primary concern, Case 1 is preferable. However, if power loss reduction and grid efficiency are crucial, Case 3 is better suited despite its higher costs. The balanced approach in Case 2 compromises cost and efficiency, making it a practical choice for FCS deployment.

TABLE V. RESULTS OF SCENARIO 1

Subcases	ω1	ω2	Power loss	*ICRI*	Objective function	Optimal FCS locations
Base	-	-	165.3674	-	-	-
S1-1	0	1	248.8810	0.4897	0.4897	15, 21, 29, 32
S1-2	0.5	0.5	199.7480	0.5081	0.3401	2, 13, 14, 15
S1-3	1	0	197.0236	0.5291	0.1607	2, 3, 14, 15

Figures 2 and 3 illustrate the voltage profile and power flow for different cases in Scenario 1. In Case 1, FCS locations are chosen based on cost-effectiveness, leading to increased power flow, voltage drops, and congestion in certain lines due to higher charging demand. While minimizing investment costs is financially advantageous, it compromises grid reliability and efficiency. In Cases 2 and 3, voltage deviations are reduced, and power flow is more balanced, alleviating some network congestion. However, Case 3 achieves the best grid performance at the highest investment cost, as FCSs are placed for optimal power loss reduction rather than cost minimization. Case 2 offers a practical balance between cost and efficiency, making it a viable solution for FCS deployment.

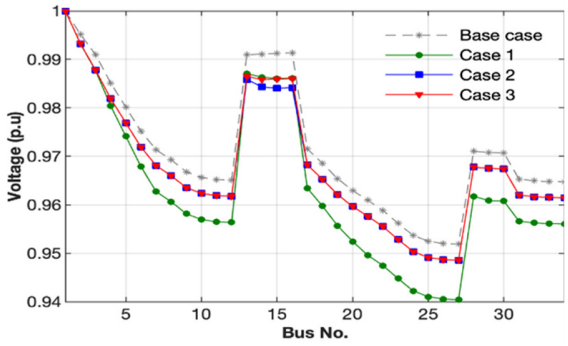

Fig. 2. Voltage profile for Scenario 1.

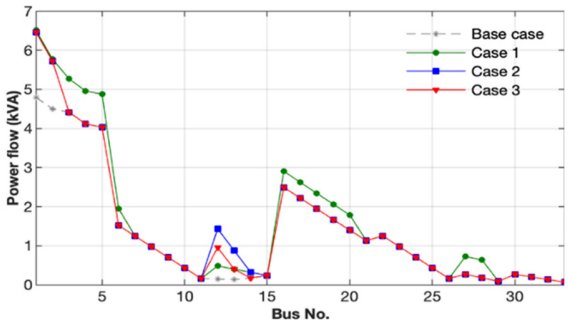

Fig. 3. Power flow for Scenario 1.

2) Scenario 2

In this scenario, EV_FCS locations are optimized using the V2G strategy. As in Scenario 1, three cases were evaluated to assess the impact of different weighting factors (ω_1 and ω_2), as shown in Table VI. The analysis of optimal EV-FCS placement reveals a trade-off between minimizing investment costs and reducing system power loss. Compared to Scenario 1, all three cases show a notable reduction in power loss, highlighting the effectiveness of V2G integration.

When prioritizing investment cost reduction (Case 1, ω_1 = 0, ω_2 = 1), power loss increases significantly to 229.7047 kW, indicating that cost-efficient locations may not enhance system efficiency. A balanced trade-off (Case 2, ω_1 = 0.5, ω_2 = 0.5) results in moderate power loss (191.1893 kW) and an *ICRI* value for investment cost (0.5081), making it a practical choice. As power loss minimization becomes dominant (Case 3, ω_1 = 1, ω_2 = 0), power loss drops further to 189.5066 kW with increased investment costs (*ICRI* value of 0.5291). Thus, investment-driven strategies lead to higher power losses, while power-loss-focused approaches require higher investments. Case 2 offers a viable compromise between these two objectives.

TABLE VI. RESULTS OF SCENARIO 2

Subcases	ω_1	ω_2	Power loss	*ICRI*	Objective function	Optimal FCS locations
Base	-	-	165.3674	-	-	-
S1-1	0	1	229.7047	0.4897	0.4897	2, 21, 29, 32
S1-2	0.5	0.5	191.1893	0.5081	0.3216	2, 13, 14, 15
S1-3	1	0	189.5066	0.5291	0.1274	2, 3, 13, 14

Figures 4 and 5 portray the voltage profile and power flow for different cases in Scenario 2 (with V2G strategy). In Case 1, voltage drops and power congestion persist in certain lines, indicating that prioritizing cost alone can still compromise grid stability despite the improvements from V2G. Cases 2 and 3 show enhanced voltage stability and a more balanced power flow distribution compared to Case 1, with reduced congestion. Case 3, however, comes with a high investment cost. Therefore, Case 2 remains the most suitable approach, providing a balance between cost and efficiency.

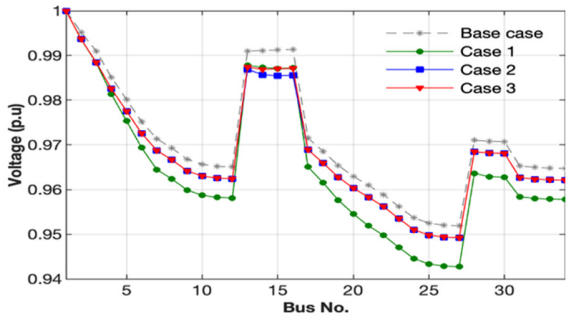

Fig. 4. Voltage profile for Scenario 2.

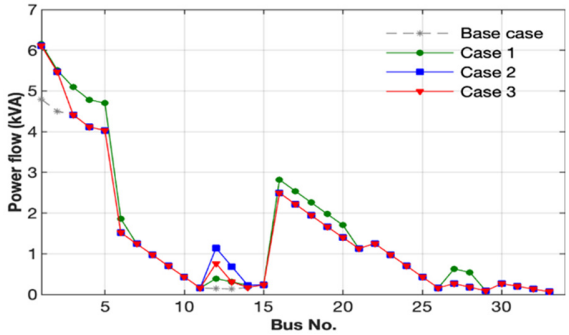

Fig. 5. Power flow for Scenario 2.

Figure 6 presents the convergence curves of EAOA for Case 2 under Scenarios 1 and 2. EAOA achieves rapid convergence in the early iterations and continues to improve gradually until around iterations 70–80, where it reaches stability. These results confirm that the selected parameters enable the algorithm to converge reliably, while maintaining a balance between exploration and exploitation.

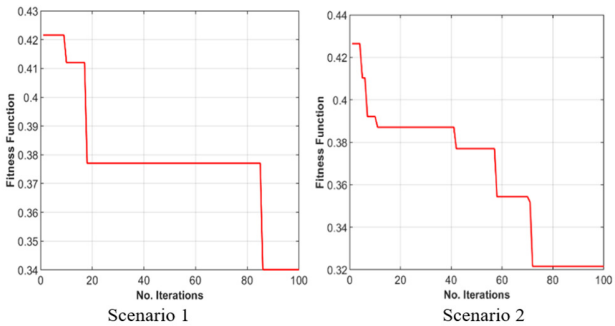

Fig. 6. Convergence curves for Case 2 of Scenarios 1 and 2.

C. Comparison with Other Methods

The proposed EAOA was compared against the GWO, as reported in [11]. With V2G integration and under the same test conditions, the proposed EAOA achieved a total installation cost of $352,517 and a real power loss of 191.1893 kW, outperforming the GWO (installation cost $361,642; power loss 207.158 kW). This corresponds to a $9,125 reduction in investment cost and a 15.97 kW reduction in power loss, highlighting EAOA's superior performance.

V. CONCLUSIONS

This study proposed a two-stage approach for optimizing Electric Vehicle Fast-Charging Stations (EV-FCS) deployment in a distribution network with renewable energy integration. Unlike previous works that focused on single or partial objectives, the proposed method combines land cost, EV population density, and Vehicle-to-Grid (V2G) integration into the optimization framework. This novelty addresses a critical gap in existing literature, where most studies optimized for either technical or economic criteria in isolation.

In the first stage, the search space was refined using the FCS owner approach, maximizing EV accessibility while minimizing land costs to reduce investment expenses. In the second stage, an EAOA was applied to determine optimal FCS placement, minimizing investment costs and power losses while ensuring voltage stability and power quality. The enhanced EAOA, strengthened with the SQI strategy, demonstrated superior performance compared to traditional metaheuristics in solving the placement problem.

The methodology was tested on the IEEE 34-bus system with solar-based Distributed Generations (DGs) under two scenarios: S-1 (without V2G) and S-2 (with V2G). The results demonstrate that V2G integration in S-2 significantly improves system performance by reducing power losses compared to S-1. Moreover, three subcases were analyzed based on different weighting factors: Case 1 led to higher power losses and voltage drops, indicating that cost-driven placement can compromise grid reliability. Case 2 achieved a moderate reduction in power loss and improved voltage stability. Case 3 resulted in the lowest power losses and the most stable voltage profile, but required the highest investment cost. Overall, the findings highlight that Case 2 provides the most practical solution, balancing investment cost and grid efficiency, while V2G plays a crucial role in reducing grid stress and enhancing power quality.

Compared with the GWO, the EAOA achieved lower power losses and investment cost, demonstrating its robustness and practicality for both planners and investors. Future EV charging infrastructure planning should incorporate V2G strategies and optimized FCS placement to improve the resilience and sustainability of modern distribution networks. Comparisons confirmed that EAOA outperforms other methods, proving its effectiveness.

ACKNOWLEDGMENT

This research is funded by Vietnam National University Ho Chi Minh City (VNU-HCM) under grant number C2024-20-35. We acknowledge Ho Chi Minh City University of Technology (HCMUT), VNU-HCM for supporting this study.

REFERENCES

[1] L. Chen, C. Xu, H. Song, and K. Jermsittiparsert, "Optimal sizing and sitting of EVCS in the distribution system using metaheuristics: A case study," *Energy Reports*, vol. 7, pp. 208–217, Nov. 2021, https://doi.org/10.1016/j.egyr.2020.12.032.

[2] Md. M. Islam, H. Shareef, and A. Mohamed, "Optimal location and sizing of fast charging stations for electric vehicles by incorporating traffic and power networks," *IET Intelligent Transport Systems*, vol. 12, no. 8, pp. 947–957, 2018, https://doi.org/10.1049/iet-its.2018.5136.

[3] A. Pal, A. Bhattacharya, and A. K. Chakraborty, "Allocation of electric vehicle charging station considering uncertainties," *Sustainable Energy, Grids and Networks*, vol. 25, Mar. 2021, Art. no. 100422, https://doi.org/10.1016/j.segan.2020.100422.

[4] G. Battapothula, C. Yammani, and S. Maheswarapu, "Multi-objective optimal planning of FCSs and DGs in distribution system with future EV load enhancement," *IET Electrical Systems in Transportation*, vol. 9, no. 3, pp. 128–139, 2019, https://doi.org/10.1049/iet-est.2018.5066.

[5] M. H. Moradi, M. Abedini, S. M. R. Tousi, and S. M. Hosseinian, "Optimal siting and sizing of renewable energy sources and charging stations simultaneously based on Differential Evolution algorithm," *International Journal of Electrical Power & Energy Systems*, vol. 73, pp. 1015–1024, Dec. 2015, https://doi.org/10.1016/j.ijepes.2015.06.029.

[6] L. Bitencourt, T. P. Abud, B. H. Dias, B. S. M. C. Borba, R. S. Maciel, and J. Quirós-Tortós, "Optimal location of EV charging stations in a neighborhood considering a multi-objective approach," *Electric Power Systems Research*, vol. 199, Oct. 2021, Art. no. 107391, https://doi.org/10.1016/j.epsr.2021.107391.

[7] J. Cheng, J. Xu, W. Chen, and B. Song, "Locating and sizing method of electric vehicle charging station based on Improved Whale Optimization Algorithm," *Energy Reports*, vol. 8, pp. 4386–4400, Nov. 2022, https://doi.org/10.1016/j.egyr.2022.03.077.

[8] C. Li, L. Zhang, Z. Ou, Q. Wang, D. Zhou, and J. Ma, "Robust model of electric vehicle charging station location considering renewable energy and storage equipment," *Energy*, vol. 238, Jan. 2022, Art. no. 121713, https://doi.org/10.1016/j.energy.2021.121713.

[9] M. S. K. Reddy and K. Selvajyothi, "Optimal placement of electric vehicle charging station for unbalanced radial distribution systems," *Energy Sources, Part A: Recovery, Utilization, and Environmental Effects*, vol. 47, no. 2, 2025, Art. no. 1731017, https://doi.org/10.1080/15567036.2020.1731017.

[10] A. Mohsenzadeh, S. Pazouki, S. Ardalan, and M.-R. Haghifam, "Optimal placing and sizing of parking lots including different levels of charging stations in electric distribution networks," *International Journal of Ambient Energy*, vol. 39, no. 7, pp. 743–750, 2018, https://doi.org/10.1080/01430750.2017.1345010.

[11] F. Ahmad, A. Iqbal, I. Ashraf, M. Marzband, and I. Khan, "Placement of Electric Vehicle Fast Charging Stations using Grey Wolf Optimization in Electrical Distribution Network," *in 2022 IEEE International Conference on Power Electronics, Smart Grid, and Renewable Energy (PESGRE)*, Thiruvananthapuram (Trivandrum), Kerala, India, Jan. 2022, pp. 1–6, https://doi.org/10.1109/PESGRE52268.2022.9715842.

[12] X. Luo and R. Qiu, "Electric vehicle charging station location towards sustainable cities," *International journal of environmental research and public health*, vol. 17, no. 8, 2020, Art. no. 2785, https://doi.org/10.3390/ijerph17082785.

[13] P. Rajesh and F. H. Shajin, "Optimal allocation of EV charging spots and capacitors in distribution network improving voltage and power loss by Quantum-Behaved and Gaussian Mutational Dragonfly Algorithm (QGDA)," *Electric Power Systems Research*, vol. 194, May 2021, Art. no. 107049, https://doi.org/10.1016/j.epsr.2021.107049.

[14] M. Bilal, M. Rizwan, I. Alsaidan, and F. M. Almasoudi, "AI-Based Approach for Optimal Placement of EVCS and DG With Reliability Analysis," *IEEE Access*, vol. 9, pp. 154204–154224, 2021, https://doi.org/10.1109/ACCESS.2021.3125135.

[15] A. N. Archana and T. Rajeev, "A Novel Reliability Index Based Approach for EV Charging Station Allocation in Distribution System," *IEEE Transactions on Industry Applications*, vol. 57, no. 6, pp. 6385–6394, Oct. 2021, https://doi.org/10.1109/TIA.2021.3109570.

[16] F. Ahmad, I. Ashraf, A. Iqbal, M. Marzband, and I. Khan, "A novel AI approach for optimal deployment of EV fast charging station and reliability analysis with solar based DGs in distribution network," *Energy Reports*, vol. 8, pp. 11646–11660, Nov. 2022, https://doi.org/10.1016/j.egyr.2022.09.058.

[17] F. Ahmad, A. Iqbal, I. Ashraf, M. Marzband, and I. Khan, "Placement of electric vehicle fast charging stations in distribution network considering power loss, land cost, and electric vehicle population," *Energy Sources, Part A: Recovery, Utilization, and Environmental Effects*, vol. 44, no. 1, pp. 1693–1709, Mar. 2022, https://doi.org/10.1080/15567036.2022.2055233.

[18] H. D. Nguyen, P. M. Le, and K. H. Truong, "Searching Optimal Placement and Operations of Energy Storage Systems based on Equilibrium Optimizer," *Engineering, Technology & Applied Science Research*, vol. 15, no. 4, pp. 24174–24180, Aug. 2025, https://doi.org/10.48084/etasr.11238.

[19] T. L. Duong and T. T. Nguyen, "Network Reconfiguration for an Electric Distribution System with Distributed Generators based on Symbiotic Organisms Search," *Engineering, Technology & Applied Science Research*, vol. 9, no. 6, pp. 4925–4932, Dec. 2019, https://doi.org/10.48084/etasr.3166.

[20] L. Abualigah, A. Diabat, S. Mirjalili, M. Abd Elaziz, and A. H. Gandomi, "The Arithmetic Optimization Algorithm," *Computer Methods in Applied Mechanics and Engineering*, vol. 376, Apr. 2021, Art. no. 113609, https://doi.org/10.1016/j.cma.2020.113609.

[21] T. H. B. Huy, T. V. Tran, D. Ngoc Vo, and H. T. T. Nguyen, "An improved metaheuristic method for simultaneous network reconfiguration and distributed generation allocation," *Alexandria Engineering Journal*, vol. 61, no. 10, pp. 8069–8088, Oct. 2022, https://doi.org/10.1016/j.aej.2022.01.056.

[22] T. V. Tran, B.-H. Truong, T. P. Nguyen, T. A. Nguyen, T. L. Duong, and D. N. Vo, "Reconfiguration of Distribution Networks With Distributed Generations Using an Improved Neural Network Algorithm," *IEEE Access*, vol. 9, pp. 165618–165647, 2021, https://doi.org/10.1109/ACCESS.2021.3134872.